EXAFS of Aqueous Pb Adsorbed underneath Fatty Acid Langmuir Monolayers

M. Boyanov,[1] J. Kmetko,[2] T. Shibata,[1] A. Datta,[2,3] B. Bunker,[1] P. Dutta[2]
[1]Department of Physics, University of Notre Dame, Notre Dame, IN, U.S.A.
[2]Department of Physics and Astronomy, Northwestern University, Evanston, IL, U.S.A.
[3]*Present address: Saha Institute of Nuclear Physics, Calcutta, India*

Introduction

There is considerable interest in the adsorption of metal cations in an aqueous solution onto Langmuir monolayers of long-chain fatty acids, both in understanding the underlying interactions that drive the metal condensation and monolayer formation and in the use of such systems as precursors to technologically useful Langmuir-Blodgett films [1]. Synchrotron grazing incidence diffraction (GID) studies revealed that ions in the subphase induce a structure in the Langmuir monolayer that is similar to the high-pressure *"S"* phase on pure water, even at low pressures. Furthermore, under certain conditions such as pH and metal concentration, a superstructure is observed. For Cd ions in the subphase, GID data from a monolayer at near zero surface pressure show diffraction peaks from an asymmetrically distorted fatty acid monolayer along with weaker peaks from a supercell of the monolayer lattice. The latter have been assigned to a monolayer of Cd ions [2]. Preliminary results from grazing incidence x-ray absorption fine structure (XAFS) of Zn ions underneath a fatty acid Langmuir monolayer indicate, among other things, a decrease in the Zn coordination number with respect to the bulk value [3], indicating a considerably different microenvironment. GID studies on heneicosanoic acid ($CH_3(CH_2)_{19}COOH$, C21 acid) on a subphase containing Zn ions show peaks only from the fatty acid monolayer [4], whereas some extra peaks similar to those observed with Cd ions are seen when Pb ions are present in the subphase [5]. Direct confirmation of the presence of the metal monolayer is lacking, as is more detailed information about the immediate environment of the metal ions.

In this study, we used grazing incidence XAFS spectroscopy at the Pb-L_{III} edge to directly detect the adsorption of Pb cations at the aqueous subphase/fatty acid monolayer interface and to provide insight into the adsorption mechanism by determining the local atomic environment of the adsorbed Pb atoms or hydrolysis complexes.

Methods and Materials

Experiments were carried out at the Materials Research Collaborative Access Team (MR-CAT) 10-ID beamline at the APS. The MR-CAT beamline is equipped with a tunable undulator and a cryogenic double-crystal Si (111) [6]. A harmonic rejection mirror was used to eliminate the third and higher x-ray harmonics from the monochromator. The Langmuir trough that was used is described in detail elsewhere [7]; it is an enclosed system with Kapton windows for the incident and scattered x-rays and with a gas inlet and outlet to maintain a slight overpressure of He. The ~10^{-4} M $PbCl_2$ solution subphase was prepared by diluting a stock solution obtained from dissolving powder $PbCl_2$ (Sigma-Aldrich) in millipore water (resistivity 18 MΩ-cm). The pH of the solutions was adjusted to 6.5 by using NaOH. The Langmuir monolayer was spread on the subphase by a microsyringe gently dropping about 65 μL of C21 acid dissolved in chloroform (0.9 mg/mL). Monolayers were compressed by a constant perimeter barrier to a slight positive surface pressure that was taken to be ~1.0 ± 0.5 dynes/cm (Balance ST9000, Nima Technology). Temperature was maintained at 9°C by circulating water.

Total external reflection geometry was employed, with the incidence angle set at 0.065°, slightly below the critical angle of water. The calculated penetration depth at this angle and at the Pb-L_{III} energy is about 100 Å. The incident x-ray beam was defined to a vertical thickness of 20 μm and a 20-mm horizontal width. Fluorescence XAFS data were collected at the Pb-L_{III} edge by using two Stern-Heald-type detectors placed above and on the side of the surface (perpendicular to the beam) and filled with Kr. The continuous scanning mode of the monochromator was used, which reduces exposure time (ca. 6 min/scan) and radiation damage. Before the XAFS experiments, GID data were collected to verify that the monolayer structure being measured was the same as the supercell structure observed in previous experiments [5].

For purposes of comparison and theory calibration in later extended XAFS (EXAFS) analysis, transmission data from several aqueous Pb solution standards were taken. As a standard for hydrated Pb cation, a 0.2 M solution of $Pb(ClO_4)_2$ at pH 2.5 was used. As a standard for the $Pb_4(OH)_4^{4+}$ hydrolysis complex, a 0.2 M solution of $Pb(ClO_4)_2$ at pH 5.8 was used. As standards for a Pb cation bound to a carboxyl group in solution, a 0.1 M

solution of $Pb(CH_3COO)_2$ $3H_2O$ with NH_3CH_3COO added to make Pb binding more probable were used. The solution standards were placed in Plexiglas slides with Kapton film windows.

Results

No edge-step was observed in the XAFS scans performed on the 10^{-4} M $PbCl_2$ subphase in grazing incidence geometry. This indicates that in the absence of the C21 monolayer, Pb atom segregation in the 100-Å-thick layer sampled by the x-rays at the interface is not measurable. Scans performed after the spreading of the C21 monolayer produced a measurable edge-step height, indicating significant Pb condensation at the interface.

GID experiments on the Pb-Langmuir monolayer system confirmed the results obtained in earlier work [5] regarding the presence of strong C21 lattice peaks and weaker peaks corresponding to a supercell structure. This GID pattern was observed to be stable for about 45 min of radiation exposure at the x-ray intensity used. Consequently, only four to five XAFS scans were performed on each sample, after which a fresh sample was prepared. This ensured that the XAFS data reflected the local environment around the Pb atoms in the structure observed by GID. The reduced $k^3\chi(k)$ EXAFS data obtained as result of averaging four to five scans/sample from seven identically prepared samples are shown in Fig. 1. The EXAFS spectra obtained from the solution standards are shown on the same figure.

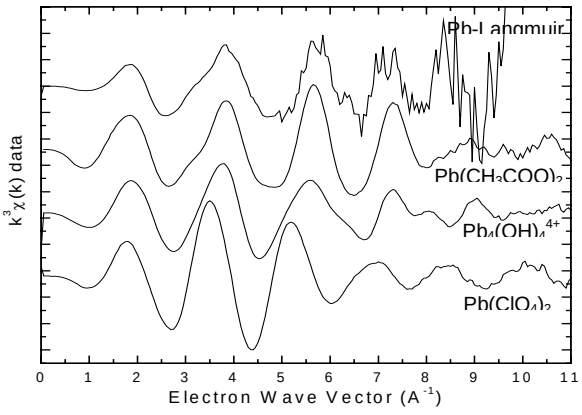

FIG. 1. $k^3\chi(k)$ EXAFS data.

Discussion

The Pb-fluorescence signal is present in this grazing-incidence geometry only when the C21 layer is spread, clearly indicating that there is significant Pb aggregation at the interface caused by the Langmuir monolayer. The XAFS result is thus a direct confirmation that electrostatic and covalent interactions of the adsorbed Pb ions or complexes with the carboxylic headgroups cause the formation of the high-pressure *"S"* phase of the Langmuir monolayer, even at zero surface pressure. A similar result was obtained from XAFS for Mn^{2+} ions [8].

Fourier transforms (FTs), Δk = [2.2-7.5] and dk = 1.0 $Å^{-1}$, of the $k^3\chi(k)$ EXAFS data for the Langmuir monolayer sample and the solution standards are shown in Fig. 2. Qualitative observation of the hydration standard [$Pb(ClO_4)_2$ solution] data indicates that the first FT peak is shifted to higher distances relative to solutions in which the Pb cation is bound. The first FT peak of the Pb-Langmuir monolayer sample data occurs at distances similar to the $Pb_4(OH)_4{}^{4+}$ and $Pb(CH_3COO)_2$ solutions data, indicating that the near-neighbor O-shell of the adsorbed Pb is consistent with bound rather than with hydrated Pb species.

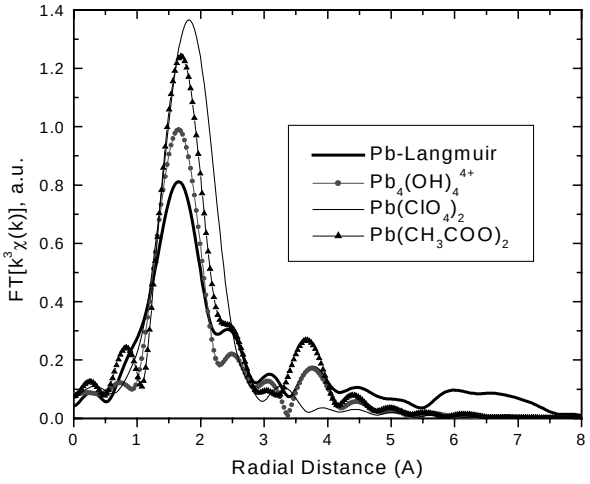

FIG. 2. Magnitude of FT of $K^3\chi(k)$ data.

Figure 3 shows FT [$k^n\chi(k)$] (n = 1, 2, 3) of the $Pb_4(OH)_4{}^{4+}$ solution standard, the Langmuir monolayer sample, and one of the $Pb(CH_3COO)_2$ solution standards. The spectra at k^2 and k^1 weightings are scaled to the peak height at k^3 weighting. Comparison between the different spectra in the region up to 2.5 Å at all k weightings shows that the near-neighbor environment in the Pb-Langmuir sample is consistent with a carboxyl environment, indicating that the Pb atoms in the monolayer are bound to the carboxyl head groups. Comparison of the region 2.5-4.5 Å shows greater similarity of the Pb-Langmuir

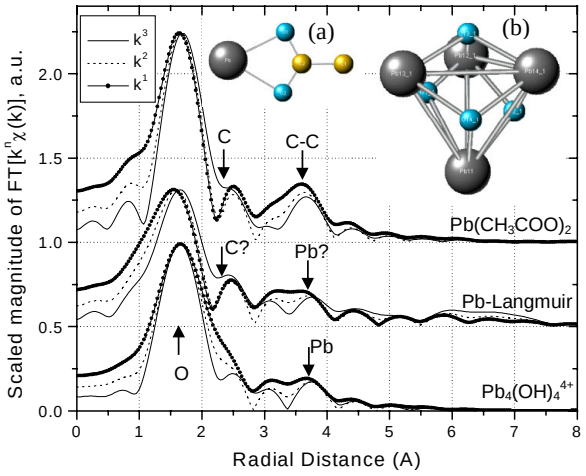

FIG. 3. Scaled $|FT[k^3\chi(k)]|$ data and structures of the aqueous Pb complexes: (a) Pb acetate and (b) $Pb_4(OH)_4^{4+}$.

sample to the $Pb_4(OH)_4^{4+}$ than to the $Pb(CH_3COO)_2$ solution standards, at all *k* weightings. The feature at 4.0 Å in the $Pb_4(OH)_4^{4+}$ spectrum is caused by the Pb-Pb interactions in the Pb_4 tetrahedron, and it indicates the presence of such interactions in the adsorbed Pb-atoms.

The qualitative analysis above suggests that the Pb atoms do not adsorb as hydrated ions but as hydrolysis products, viz. $Pb_4(OH)_4^{4+}$. Furthermore, the features in the FT at small distances (up to 2.5 Å) suggest that the majority of the probed Pb atoms are bound to carboxyl groups. This is consistent with the Pb_4 tetrahedron being oriented with one face toward the C21 monolayer and the three Pb atoms at the corners being bound to the carboxyl headgroups. The C21 lattice spacing and the tetrahedron side in $Pb_4(OH)_4^{4+}$ are similar in size, allowing such binding. The charge around a "plane-adsorbed" complex would be +1 (equals +4 – [1 × 3]) and an attraction center for the neighboring negatively charged carboxyl groups, facilitating the formation of the close-packed structure. The large supercell area (14 times the C21 monolayer cell) observed in the GID experiments [5] could also be explained better by a large-area adsorption mode such as the one proposed. The superstructure layer thickness of ca. 5 Å determined from Bragg-rod scans of the diffraction peaks [5] is consistent with the dimensions of such an adsorption complex. Precise structural information from the detailed fitting analysis underway will give more insight into the exact binding mechanism.

A complication that arises in the analysis is the polarization dependence of the EXAFS. The x-ray beam is polarized in the plane of the Langmuir monolayer, and the monolayer itself is a 2-D powder consisting of small "crystalline" domains oriented randomly in the plane. Preliminary model calculations indicate that the carboxyl group contribution to the EXAFS is enhanced when the Pb-C-C axis is parallel to the polarization plane and suppressed when the Pb atom is situated directly below the carboxyl group (Pb-C-C axis perpendicular to the polarization plane). A similar effect is observed for the signal at 4.0 Å in the $Pb(CH_3COO)_4$ solution standards; it was traced to C-C multiple scattering. Conversely, practically no polarization dependence is observed when the Pb-Pb interaction is modeled in $Pb_4(OH)_4^{4+}$ because of the higher symmetry of this cluster and the averaging over the orientation of all four Pb atoms. The two results above can help explain the reduced first-peak amplitude in Fig. 2 of the Pb-Langmuir FT spectra relative to the $Pb_4(OH)_4^{4+}$ and $Pb(CH_3COO)_2$ solution standards and also the lack, or small contribution, of the C-C multiple scattering to the spectra at 4.0 Å.

Acknowledgments

M. Boyanov wishes to thank the Bayer Corporation for its support through the Bayer predoctoral fellowship. Beamline alignment help from the staff of MR-CAT is greatly appreciated. MR-CAT is supported by the U.S. Department of Energy (DOE) under Contract DE-FG02-94-ER45525 and the member institutions. Use of the APS was supported by the DOE Office of Science, Office of Basic Energy Sciences, under Contract No. W-31-102-ENG-38.

References

[1] A. Ulman, *An Introduction to Ultrathin Organic Films from Langmuir-Blodgett to Self Assembly* (Academic Press, New York, N.Y., 1991).

[2] C. Böhm, F. Leveiller, D. Jacquemain, H. Mohwald, K. Kjaer, J. Alsnielsen, I. Weissbuch, and L. Leiserowirz, Langmuir **10**, 830-836 (1994).

[3] I. Watanabe, H. Tanida, and S. Kawauchi, J. Am. Chem. Soc. **119**(49), 12018-12019 (1997).

[4] A. Datta, J. Kmetko, C.-J. Yu, A. G. Richter, and P. Dutta, J. Phys. Chem. B **104**, 5797 (2000).

[5] J. Kmetko, A. Datta, G. Evmenenko, and P. Dutta, J. Phys. Chem. **105**(44), 10818-10825 (2001).

[6] C. Segre, N. Leyarovska, L. Chapman, W. Lavender, P. Plag, A. King, A. Kropf, B. Bunker, K. Kemner, P. Dutta, R. Duran, and J. Kaduk, Synch. Rad. Instrum. **CP521**, 419-422 (2000).

[7] S. Barton, B. Thomas, S. Rice, B. Lin, J. Peng, J. Ketterson, P. Dutta, J. Chem. Phys. **89**, 2257-2270 (1988).

[8] J. Bloch, W. Yun, X. Yang, M. Ramanathan, P. Montano, C. Capasso, Phys. Rev. Lett. **61**(26), 2941-2944 (1988).